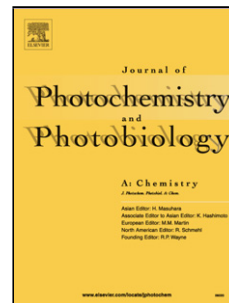


# Journal Pre-proof

Design and synthesis of a solvent-dependent fluorescent probe for dual selective detection of Mg<sup>2+</sup> ion and Zn<sup>2+</sup> ion

Jing-Can Qin (Investigation) (Methodology) (Data curation) (Writing - original draft), Min Wang (Investigation) (Software) (Writing - review and editing), Zhen-Hai Fu (Supervision) (Writing - review and editing), Zhi-Hong Zhang (Project administration)



PII: S1010-6030(20)30762-0

DOI: <https://doi.org/10.1016/j.jphotochem.2020.112965>

Reference: JPC 112965

To appear in: *Journal of Photochemistry & Photobiology, A: Chemistry*

Received Date: 22 July 2020

Revised Date: 19 September 2020

Accepted Date: 1 October 2020

Please cite this article as: { doi: <https://doi.org/>

This is a PDF file of an article that has undergone enhancements after acceptance, such as the addition of a cover page and metadata, and formatting for readability, but it is not yet the definitive version of record. This version will undergo additional copyediting, typesetting and review before it is published in its final form, but we are providing this version to give early visibility of the article. Please note that, during the production process, errors may be discovered which could affect the content, and all legal disclaimers that apply to the journal pertain.

© 2020 Published by Elsevier.

**Design and synthesis of a solvent-dependent fluorescent probe for dual selective detection of Mg<sup>2+</sup> ion and Zn<sup>2+</sup> ion**

Jing-Can Qin,<sup>a,b</sup> Min, Wang,<sup>a,b,c</sup> Zhen-Hai Fu,<sup>\*a,b,d</sup> Zhi-Hong Zhang<sup>a,b,d</sup>

a. Key Laboratory of Comprehensive and Highly Efficient Utilization of Salt Lake Resources, Qinghai Institute of Salt Lakes, Chinese Academy of Sciences, Xining, 810008, People's Republic of China.

b. Key Laboratory of Salt Lake Resources Chemistry of Qinghai Province, Xining, 810008, People's Republic of China.

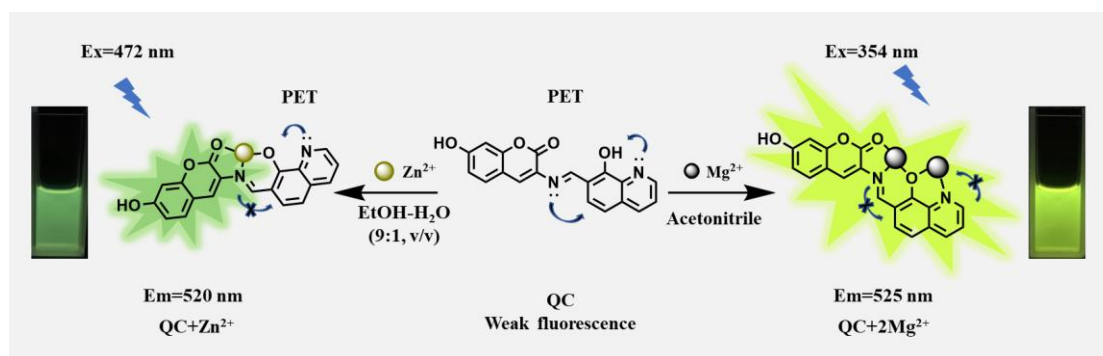
c. University of Chinese Academy of Sciences, Beijing, 100049, People's Republic of China.

d. Innovation academy for green Manufacture, Chinese Academy of Sciences, Beijing, 100049, People's Republic of China.

E-mail for corresponding author: fzh@isl.ac.cn (Z.-H. Fu)

Corresponding author: Zhen-Hai Fu

**Graphical Abstract**



### Highlights

- 8-hydroxyquinoline in probe served as not only a fluorophore but also a recognition site.
- The detection of Mg<sup>2+</sup> ion was achieved in acetonitrile.
- The detection of Zn<sup>2+</sup> ion was achieved in EtOH-H<sub>2</sub>O (9:1, v/v).

### Abstract

A solvent-dependent fluorescent probe **QC** for the dual detection of Mg<sup>2+</sup> ion and Zn<sup>2+</sup> ion has been constructed based on a Schiff base compound, in which 8-hydroxyquinoline served as not only a fluorophore but also a recognition group. Among the various tested metal ions, this probe exhibited high sensitivity and good selectivity toward Mg<sup>2+</sup> ion in acetonitrile and Zn<sup>2+</sup> ion in EtOH-H<sub>2</sub>O (9:1, v/v), respectively. With the treatment of Mg<sup>2+</sup> ion or Zn<sup>2+</sup> ion, 1:2 complex was formed between **QC** and Mg<sup>2+</sup> ion, which inhibited the PET processes caused by the lone pair electrons from the nitrogen atom of the -C=N group and the nitrogen atom of quinoline moiety, resulting in the fluorescence enhancement for Mg<sup>2+</sup> ion. Whereas a 1:1 complex was formed between **QC** and Zn<sup>2+</sup> ion, which inhibited the PET process only caused by the lone pair electrons from the nitrogen atom of the -C=N group, resulting in the fluorescence

enhancement at a shorter wavelength. The detection limit was calculated as low as  $6.28 \times 10^{-8}$  M for  $\text{Mg}^{2+}$  ion and  $2.36 \times 10^{-7}$  M for  $\text{Zn}^{2+}$  ion. DFT analysis further supported this concept to design the probe.

**Keywords:** Fluorescence, Quinoline, Coumarin,  $\text{Mg}^{2+}$  and  $\text{Zn}^{2+}$

## 1. Introduction

As we known that  $\text{Mg}^{2+}$  ion is the most abundant divalent cations in living beings and environments, it not only performs great functions in many biochemical processes, but also contributes to the productivity and quality of agriculture as a nutrient element [1,2]. Abnormal levels of  $\text{Mg}^{2+}$  ion can cause various diseases, such as hypocalcaemia, osteoporosis, metabolic syndrome, diabetes, hypertension, hypermagnesemia, nausea, hypotension, diarrhea, Alzheimer's disease and so on [3-6].  $\text{Zn}^{2+}$  ion, as an essential transition metal nutrient, also play an important role for humans, living cells and plants. Similarly, it is also associated with some neurological diseases including Alzheimer's disease, amyotrophic lateral sclerosis, Parkinson's disease, and epilepsy [7-9]. Therefore, it is highly desirable to develop probe for the detection of  $\text{Mg}^{2+}$  ion and  $\text{Zn}^{2+}$  ion with reliable and efficient way.

over the past few years, numerous fluorescent probes have been developed [10], especially bifunction probes which have attracted great attention due to their ability to detect one more analyte beside  $\text{Mg}^{2+}$  ion or  $\text{Zn}^{2+}$  ion [11-13], which are more efficient compared with the traditional one-to-one probes. As a result, a series of such

multianalyte fluorescent probes based on Schiff base scaffold have been reported for the detection of  $\text{Zn}^{2+}$  and  $\text{Al}^{3+}$  [14],  $\text{Zn}^{2+}$  and  $\text{Bi}^{3+}$  [15],  $\text{Zn}^{2+}$  and  $\text{Cu}^{2+}$  [16],  $\text{Zn}^{2+}$  and  $\text{Fe}^{3+}$  [17],  $\text{Zn}^{2+}$  and  $\text{Hg}^{2+}$  [18],  $\text{Mg}^{2+}$  and  $\text{Fe}^{3+}$  [19],  $\text{Zn}^{2+}$ ,  $\text{Cu}^{2+}$  and  $\text{Hg}^{2+}$  [20],  $\text{Zn}^{2+}$ ,  $\text{Mg}^{2+}$  and  $\text{Al}^{3+}$  [21]. However, there are very limited probes for dual detection of  $\text{Zn}^{2+}$  ion and  $\text{Mg}^{2+}$  ion with a single probe [22-27]. As summarized in Table S1, these probes can detect them by using the difference of the fluorescence intensity or the fluorescence emission wavelength. Probes depend on fluorescence emission at different wavelength are better than those by using only fluorescence emission at one wavelength, which can be realized by controlling the solvents. Nonetheless, the sensitivity (detection limit) still needs to be improved for both  $\text{Mg}^{2+}$  ion and  $\text{Zn}^{2+}$  ion with a multianalyte fluorescent probe.

As a continuation of our research probes for the detection of different analytes [28, 29], herein, we designed and synthesized a new quinoline-based fluorescent probe **QC**, in which 8-hydroxyquinoline was used as not only a fluorophore but also a recognition site. The free probe with weak luminescence was constructed due to the C=N isomerization and the PET (photoinduced electron transfer) process. The detection of  $\text{Mg}^{2+}$  ion or  $\text{Zn}^{2+}$  ion can be realized via different binding stoichiometries and binding sites in different solvents. As a solvent-dependent fluorescent probe, the solvent influence must play an important role in the fluorescence detection of  $\text{Mg}^{2+}$  or  $\text{Zn}^{2+}$ . According to basic chemistry,  $\text{Mg}^{2+}$  is a hard acid, and it is easier to combine with oxygen (hard base). Considering that the water molecule can act as a ligand to compete with probe, so acetonitrile was selected for the detection of  $\text{Mg}^{2+}$ . Conversely, the

presence of a little water is beneficial to the fluorescence recognition of  $\text{Zn}^{2+}$ . Finally, probe exhibited highly selective detection of  $\text{Mg}^{2+}$  ion in acetonitrile and  $\text{Zn}^{2+}$  ion in EtOH- $\text{H}_2\text{O}$  (9:1, v/v), respectively.

## 2. Experimental section

### 2.1 General information

The chemicals in experiments were commercially available and used without further purification. All of solvents used in experiments were analytical-reagent grade.  $^1\text{H}$ ,  $^{13}\text{C}$  NMR spectra were measured on the JEOL JNM-ECS 400 MHz instruments using TMS as an internal standard. UV-vis spectra were performed on PerkinElmer UV/VIS/NIR Spectrometer Lambda 750. Fluorescence spectra were recorded on a SHIMADZU RF-5301 fluorescence spectrophotometer.

Various stock solutions of metal ions ( $\text{Ag}^+$ ,  $\text{K}^+$ ,  $\text{Li}^+$ ,  $\text{Na}^+$ ,  $\text{Ca}^{2+}$ ,  $\text{Hg}^{2+}$ ,  $\text{Mg}^{2+}$ ,  $\text{Mn}^{2+}$ ,  $\text{Ba}^{2+}$ ,  $\text{Cd}^{2+}$ ,  $\text{Cr}^{3+}$ ,  $\text{Pb}^{2+}$ ,  $\text{Zn}^{2+}$ ) were prepared in EtOH. Stock solutions of probe **QC** were prepared in DMSO. Test solutions were prepared by placing appropriate amount of the probe stock solution into a test tube, and then diluting to 2.0 mL with acetonitrile or EtOH- $\text{H}_2\text{O}$  (9:1, v/v), followed by the addition of an appropriate aliquot of each stock solution of metal ions. Other details of chemicals, materials and spectra measurement can be found in the Supplementary Material.

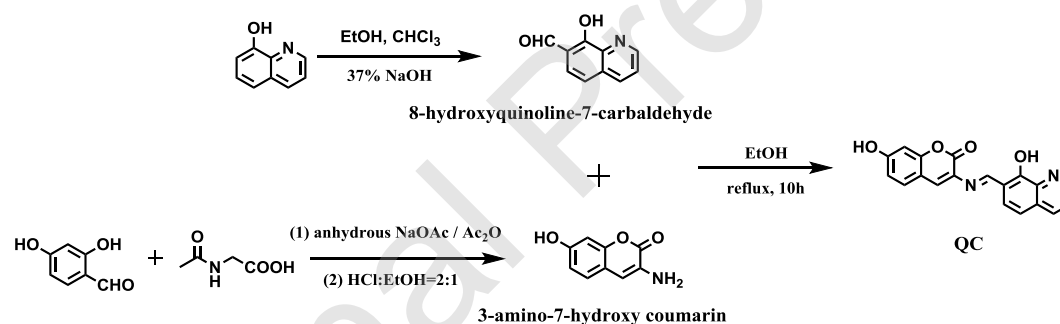
### 2.2 Synthesis of **QC** ((E)-7-hydroxy-3-(((8-hydroxyquinolin-7-yl)methylene)amino)-2H-chromen-2-one)

A mixture of 8-hydroxyquinoline-7-carbaldehyde (1.0 mmol, 0.173 g) and 3-amino-7-hydroxy coumarin (1.0 mmol, 0.177g) was dissolved in 20 mL ethanol, and then the

mixture was stirred and refluxed for 10 h. The precipitate was filtered and washed three times with ethanol (3×10 mL). The final product was dried in vacuo to afford red powder (471.9 mg, 71%). M.P.: above 300°C, <sup>1</sup>H NMR (400 MHz; DMSO-*d*<sub>6</sub>): δ = 13.13 (s, 1H), 10.46 (s, 1H), 9.34 (s, 1H), 8.88 (dd, *J* = 4.4, 1.6 Hz, 1H), 8.26 (dd, *J* = 8.4, 1.6 Hz, 1H), 8.05 (s, 1H), 7.72 (d, *J* = 8.8 Hz, 1H), 7.61 (dd, *J* = 8.4, 4.4 Hz, 1H), 7.57 (d, *J* = 8.4 Hz, 1H), 7.29 (d, *J* = 8.8 Hz, 1H), 6.86 (dd, *J* = 8.4, 5.0 Hz, 1H), 6.79 (d, *J* = 2.0 Hz, 1H) ppm. <sup>13</sup>C NMR (DMSO-*d*<sub>6</sub>, 100 MHz) δ = 160.9, 158.5, 157.9, 153.4, 148.8, 140.8, 135.9, 131.6, 129.9, 129.7, 127.9, 127.8, 127.1, 124.1, 116.8, 115.8, 113.8, 111.7, 102.1 ppm. ESI-MS: *m/z* 333.1 [M + H]<sup>+</sup>.

### 3. Results and discussion

#### 3.1 Design and syntheses of probe QC



Scheme 1. Synthesis of probe QC

As seen in Scheme 1, Fluorescent probe QC was synthesized from monoaldehyde-functionalized 8-hydroxyquinoline and 3-amino-7-hydroxy coumarin, which was confirmed by <sup>1</sup>H NMR, <sup>13</sup>C NMR and ESI-MS (Figure S1–S4, ESI<sup>†</sup>). In the design concept, 8-hydroxyquinoline was used as not only a fluorophore but also a recognition site [30], through a simple condensation reaction with 3-amino-7-hydroxy coumarin, this probe could have a new ability to chelate with different analytes.

## 3.2 Fluorescence spectra of probe QC toward metal ions

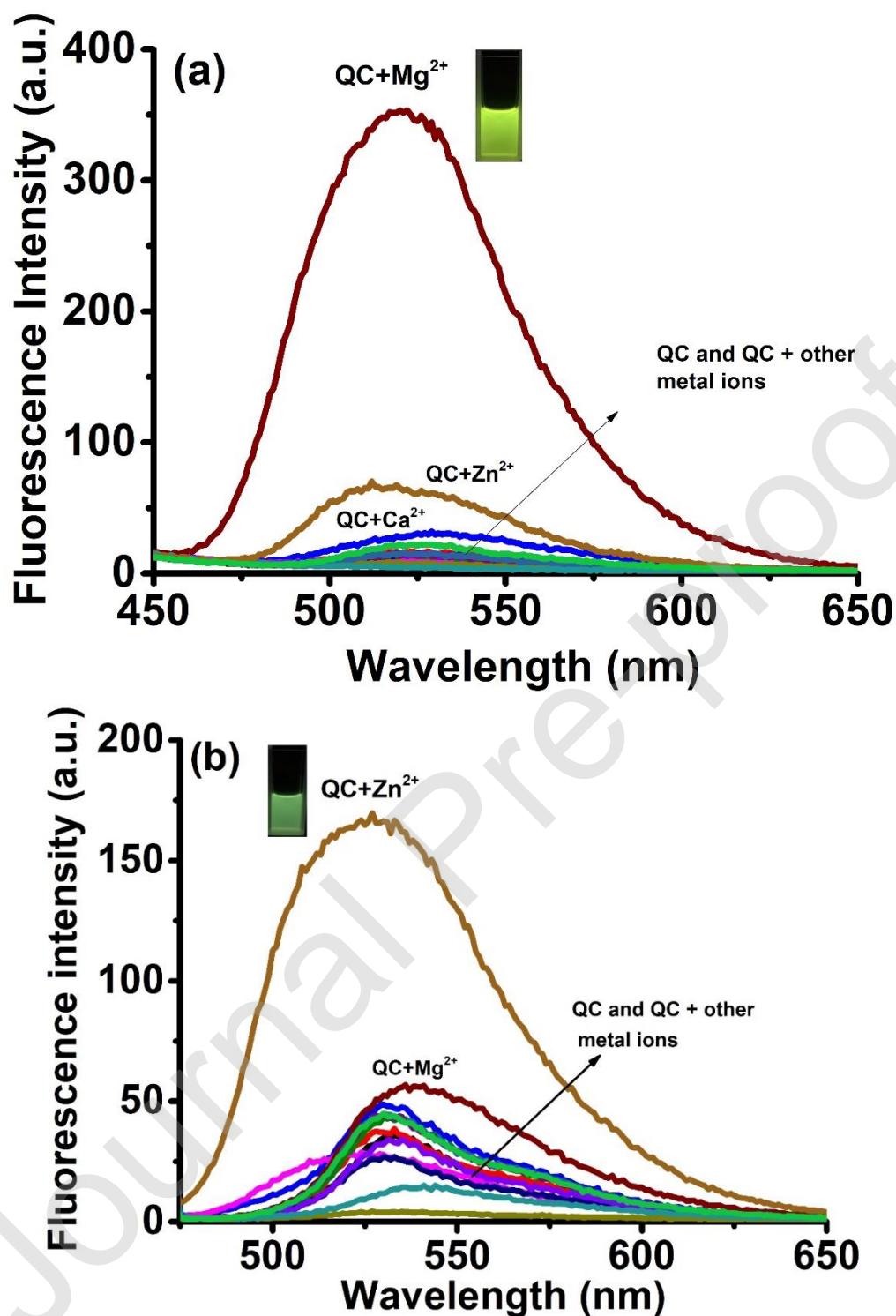
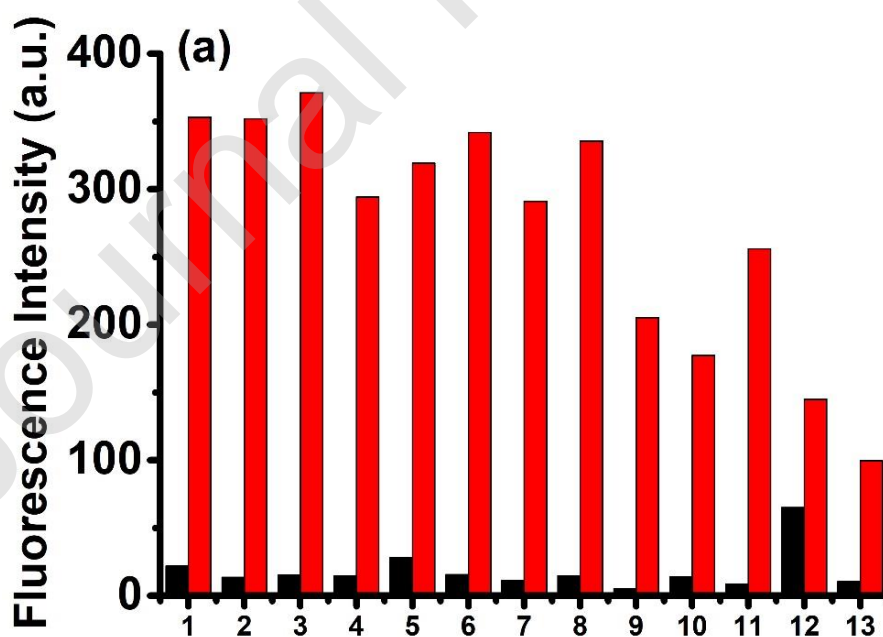


Figure 1. (a) Fluorescence responses of QC (2.0  $\mu\text{M}$ ) toward various metal ions (5.0  $\mu\text{M}$ ) in acetonitrile:  $\lambda_{\text{ex}} = 354$  nm; (b) Fluorescence responses of QC (10.0  $\mu\text{M}$ ) toward various metal ions (25.0  $\mu\text{M}$ ) in EtOH-H<sub>2</sub>O (9:1, v/v):  $\lambda_{\text{ex}} = 472$  nm.

To investigate the selectivity of **QC** for metal ions, the fluorescence spectra of **QC** against various ions including  $\text{Li}^+$ ,  $\text{Na}^+$ ,  $\text{K}^+$ ,  $\text{Mg}^{2+}$ ,  $\text{Ca}^{2+}$ ,  $\text{Ba}^{2+}$ ,  $\text{Ag}^+$ ,  $\text{Hg}^{2+}$ ,  $\text{Pb}^{2+}$ ,  $\text{Cr}^{3+}$ ,  $\text{Mn}^{2+}$ ,  $\text{Zn}^{2+}$  and  $\text{Cd}^{2+}$  were initially carried out in acetonitrile and EtOH- $\text{H}_2\text{O}$  (9:1, v/v), respectively. As demonstrated in Figure 1, it is noted that **QC** exhibited weak fluorescence peak at about 525 nm in acetonitrile due to the isomerization of C=N double bond in the excited state, and a remarkable fluorescence enhancement was observed only in the presence of  $\text{Mg}^{2+}$  ion, which inhibited the C=N isomerization, resulting in the chelation-enhanced fluorescence (CHEF) between **QC** and  $\text{Mg}^{2+}$  ion. However, As shown in Figure 1b, **QC** exhibited weak fluorescence peak at about 530 nm in EtOH- $\text{H}_2\text{O}$  (9:1, v/v), upon the addition of various tested metal ions into the solution of **QC**, a new fluorescence peak at 520 nm was observed in the treatment of  $\text{Zn}^{2+}$  ion compared to other ions including  $\text{Mg}^{2+}$  ion, which suggested that a new complex formed between **QC** and  $\text{Zn}^{2+}$  ion.



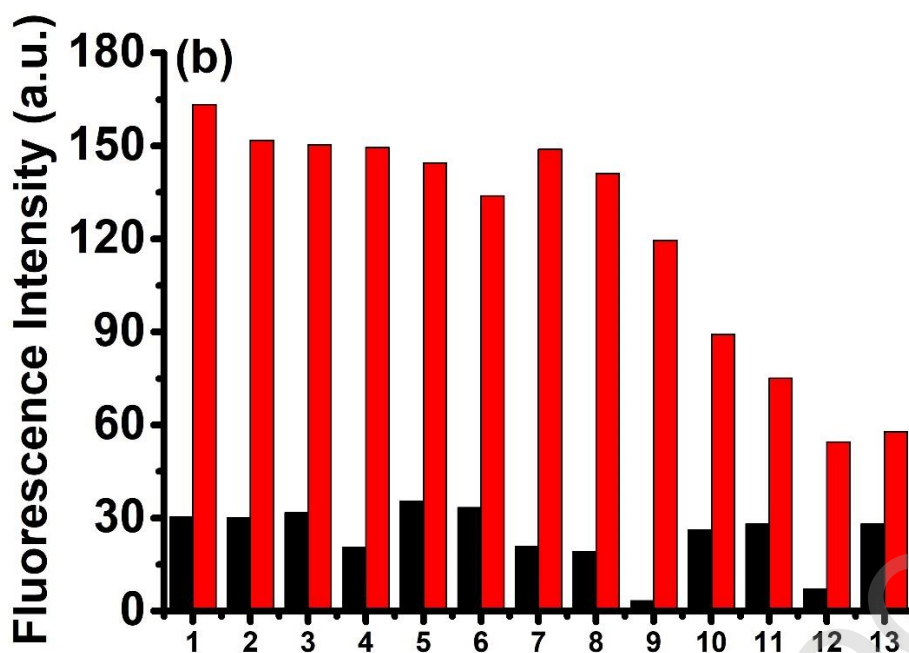


Figure 2. (a) The selectivity of **QC** ( $2.0 \mu\text{M}$ ) in acetonitrile: From 1–13: none,  $\text{Li}^+$ ,  $\text{Na}^+$ ,  $\text{K}^+$ ,  $\text{Ca}^{2+}$ ,  $\text{Ba}^{2+}$ ,  $\text{Ag}^+$ ,  $\text{Hg}^{2+}$ ,  $\text{Pb}^{2+}$ ,  $\text{Cr}^{3+}$ ,  $\text{Mn}^{2+}$ ,  $\text{Zn}^{2+}$ ,  $\text{Cd}^{2+}$ . ( $\lambda_{\text{ex}} = 354 \text{ nm}$ ); (b) The selectivity of probe **QC** ( $10.0 \mu\text{M}$ ) in EtOH- $\text{H}_2\text{O}$  (9:1, v/v): From 1–13: none,  $\text{Li}^+$ ,  $\text{Na}^+$ ,  $\text{K}^+$ ,  $\text{Ca}^{2+}$ ,  $\text{Mg}^{2+}$ ,  $\text{Ag}^+$ ,  $\text{Hg}^{2+}$ ,  $\text{Mn}^{2+}$ ,  $\text{Ba}^{2+}$ ,  $\text{Cd}^{2+}$ ,  $\text{Pb}^{2+}$ ,  $\text{Cr}^{3+}$ . ( $\lambda_{\text{ex}} = 472 \text{ nm}$ ). The black bars represent the emission intensity of **QC** in the presence of other ions; the red bars represent the emission intensity that occurs upon the subsequent addition of  $5.0 \mu\text{M}$   $\text{Mg}^{2+}$  ion or  $25.0 \mu\text{M}$   $\text{Zn}^{2+}$  ion to the above solution.

In order to check the selectivity of **QC** for  $\text{Mg}^{2+}$  ion or  $\text{Zn}^{2+}$  ion, the fluorescence response of **QC** toward them in the presence of other tested metal ions was then studied in acetonitrile and EtOH- $\text{H}_2\text{O}$  (9:1, v/v), respectively. As shown in Figure 2a and 2b,  $\text{Mg}^{2+}$  ion or  $\text{Zn}^{2+}$  ion was added into the mixture of **QC** and other tested metal ions, fluorescence enhancement still occurred both in the above solvents, which indicated that the presence of these co-existent metal cations did not interfere with the fluorescence response of **QC** toward  $\text{Mg}^{2+}$  ion or  $\text{Zn}^{2+}$  ion. These results suggested that

QC could serve as a solvent-dependent fluorescent probe for dual selective detection of  $\text{Mg}^{2+}$  ion or  $\text{Zn}^{2+}$  ion.

### 3.3 Titration of probe QC with $\text{Mg}^{2+}$ ion and $\text{Zn}^{2+}$ ion

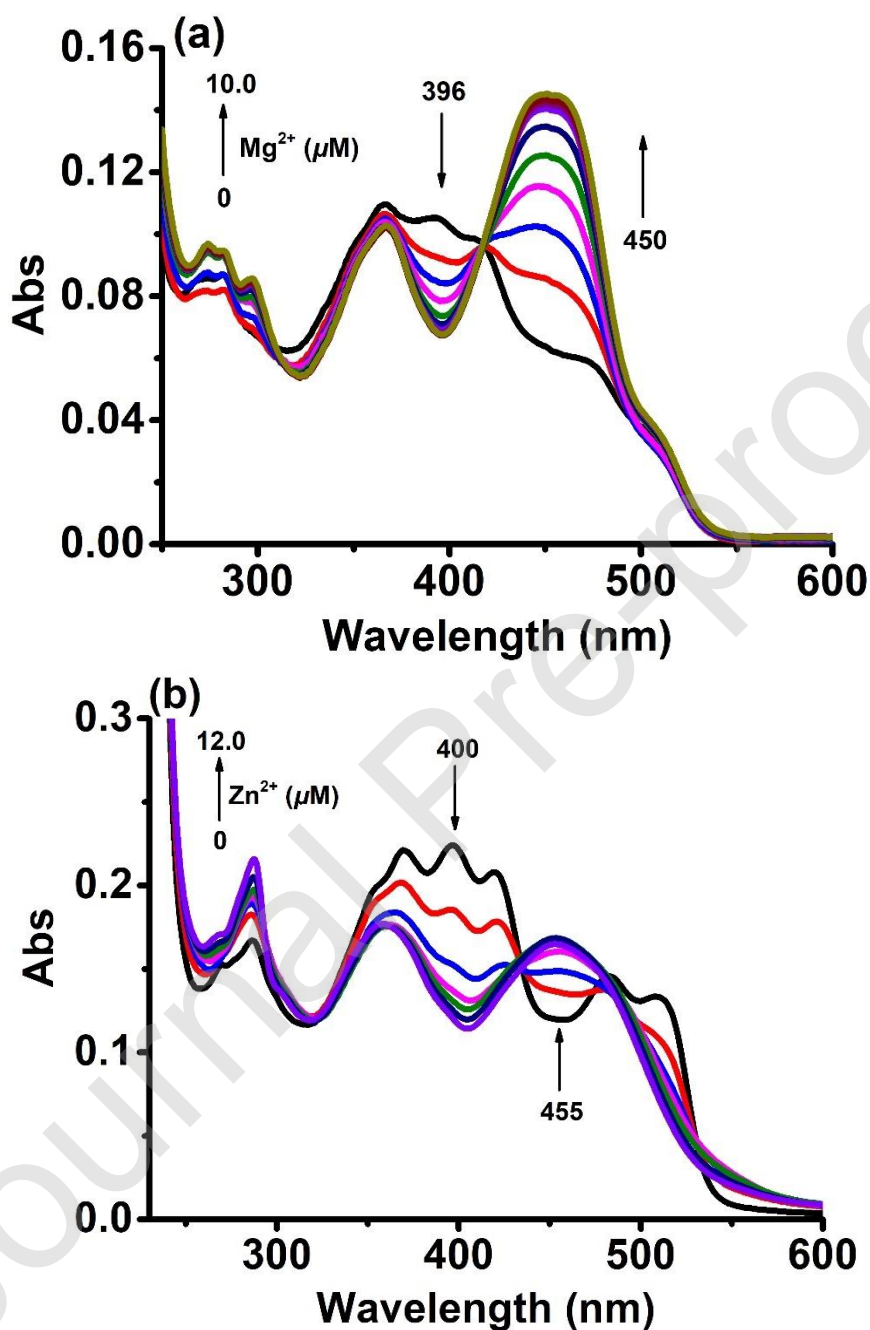
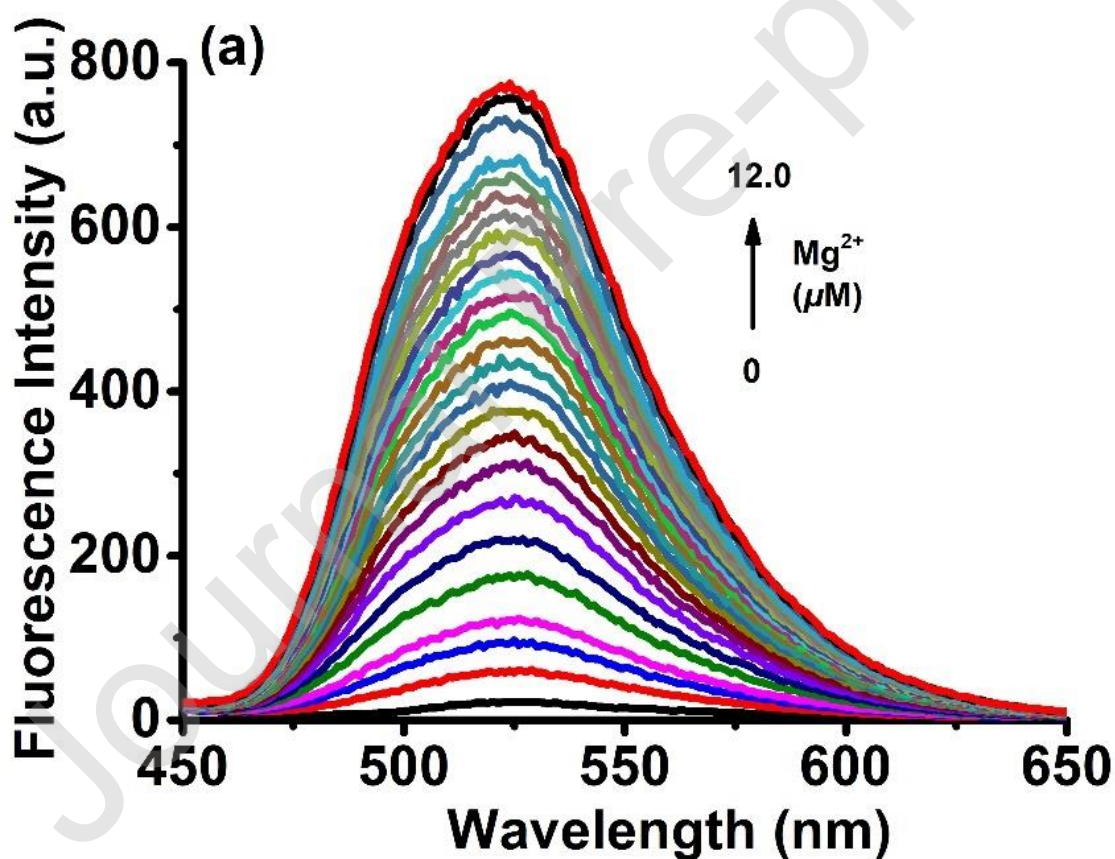


Figure 3. (a) Changes in UV-vis spectra of QC (5.0  $\mu\text{M}$ ) in acetonitrile as a function of added  $\text{Mg}^{2+}$  (0–10.0  $\mu\text{M}$ ). (b) Change in UV-vis spectra of QC (10.0  $\mu\text{M}$ ) in EtOH-H<sub>2</sub>O (9:1, v/v) as a function of added  $\text{Zn}^{2+}$  (0–12.0  $\mu\text{M}$ ).

It is well known that the titration is an important method to understand the sensitivity of probe toward analyte. Therefore, the UV- vis spectra response of QC toward  $Mg^{2+}$  ion or  $Zn^{2+}$  ion was initially carried out in acetonitrile or EtOH- $H_2O$  (9:1, v/v). As shown in Figure 3, the absorption peak of QC was distributed in a wide wavelength range from 330 nm to 550 nm. Upon the addition of  $Mg^{2+}$  ion or  $Zn^{2+}$  ion, the maximum absorption bands gradually decreased while a new absorption band appeared at about 450 nm or 455 nm with increasing intensity, and a clear isosbestic point at about 420 nm was observed, which indicated the formation of new complex between QC and  $Mg^{2+}$  ion or  $Zn^{2+}$  ion.



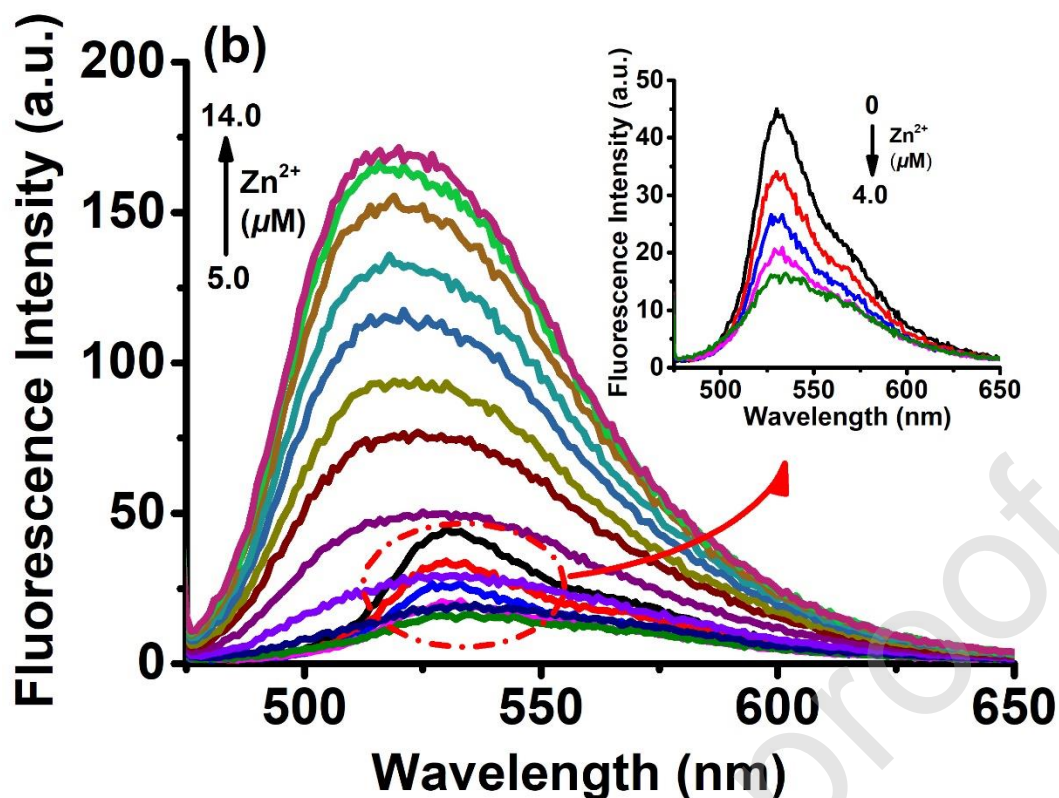


Figure 4. (a) Fluorescence spectral changes of probe **QC** ( $5.0 \mu\text{M}$ ) with the addition of  $\text{Mg}^{2+}$  ion ( $0\text{--}12.0 \mu\text{M}$ ) in acetonitrile.  $\lambda_{\text{ex}} = 354 \text{ nm}$ ; (b) Fluorescence spectral changes of probe **QC** ( $10.0 \mu\text{M}$ ) with the addition of  $\text{Zn}^{2+}$  ion ( $0\text{--}14.0 \mu\text{M}$ ) in EtOH- $\text{H}_2\text{O}$  ( $9:1, \text{v/v}$ ).  $\lambda_{\text{ex}} = 472 \text{ nm}$ .

Next, the fluorescence titrations of **QC** with  $\text{Mg}^{2+}$  ion or  $\text{Zn}^{2+}$  ion were carried out to investigate its sensitivity in acetonitrile or EtOH- $\text{H}_2\text{O}$  ( $9:1, \text{v/v}$ ). As shown in Figure 4a, by increasing addition of the  $\text{Mg}^{2+}$  concentration in acetonitrile, fluorescence intensity at  $525 \text{ nm}$  was increased gradually. Consequently, a direct linear relationship was observed between the fluorescence intensity at  $525 \text{ nm}$  and the  $\text{Mg}^{2+}$  concentration in range of  $0\text{--}5.0 \mu\text{M}$ , and the detection limit for  $\text{Mg}^{2+}$  ion was evaluated as  $6.28 \times 10^{-8} \text{ M}$  ( $\text{DL}=3\sigma/k$  ( $\text{S/N}=3$ )) (Figure S5) [31]. However, when the solvent was changed to EtOH- $\text{H}_2\text{O}$  ( $9:1, \text{v/v}$ ), upon the addition of  $\text{Zn}^{2+}$  ion, the fluorescence intensity of **QC**

decreased gradually at 530 nm and the fluorescence intensity of **QC-Zn<sup>2+</sup>** increased gradually with a slightly blue shift. A direct linear response between the fluorescence intensity at 520 nm and the **Zn<sup>2+</sup>** ion concentration range of 5–14.0  $\mu\text{M}$  was also observed, and the detection limit for **Zn<sup>2+</sup>** ion was then evaluated as low as  $2.36 \times 10^{-7}$  M by the similar way (Figure S6). The detection limit for **Mg<sup>2+</sup>** ion or **Zn<sup>2+</sup>** ion is much lower than those reported previously.

### 3.4 Binding stoichiometry and binding site

In order to investigate the binding stoichiometry between **QC** and **Mg<sup>2+</sup>** ion or **Zn<sup>2+</sup>** ion in above tested solvents, the job's plots experiments were performed and the results are shown in Figure 5. As can be seen from the Figure 5a, an inflection point was clearly observed at about 0.33 M fraction of **QC**, suggesting the formation of a complex with 1:2 stoichiometric ratio of **QC-2Mg<sup>2+</sup>** in acetonitrile. However, in EtOH-H<sub>2</sub>O (9:1, v/v), a maximum intensity at a molar fraction of 0.5 was observed for **Zn<sup>2+</sup>** ion (Figure 5b), indicating the formation of a 1:1 complex between **QC** and **Zn<sup>2+</sup>** ion. As well known that 8-hydroxyquinoline is a good chelator for **Mg<sup>2+</sup>** ion [32], and Schiff base compounds are often used to develop fluorescent probes for **Zn<sup>2+</sup>** ion [33]. Consequently, we proposed that **Mg<sup>2+</sup>** ion and **Zn<sup>2+</sup>** ion should coordinate with -OH of the quinoline moiety, -C=O of coumarin group and -C=N group of **QC** in their own complex, while one extra **Mg<sup>2+</sup>** ion also can coordinate with OH and N of the quinoline moiety in acetonitrile.

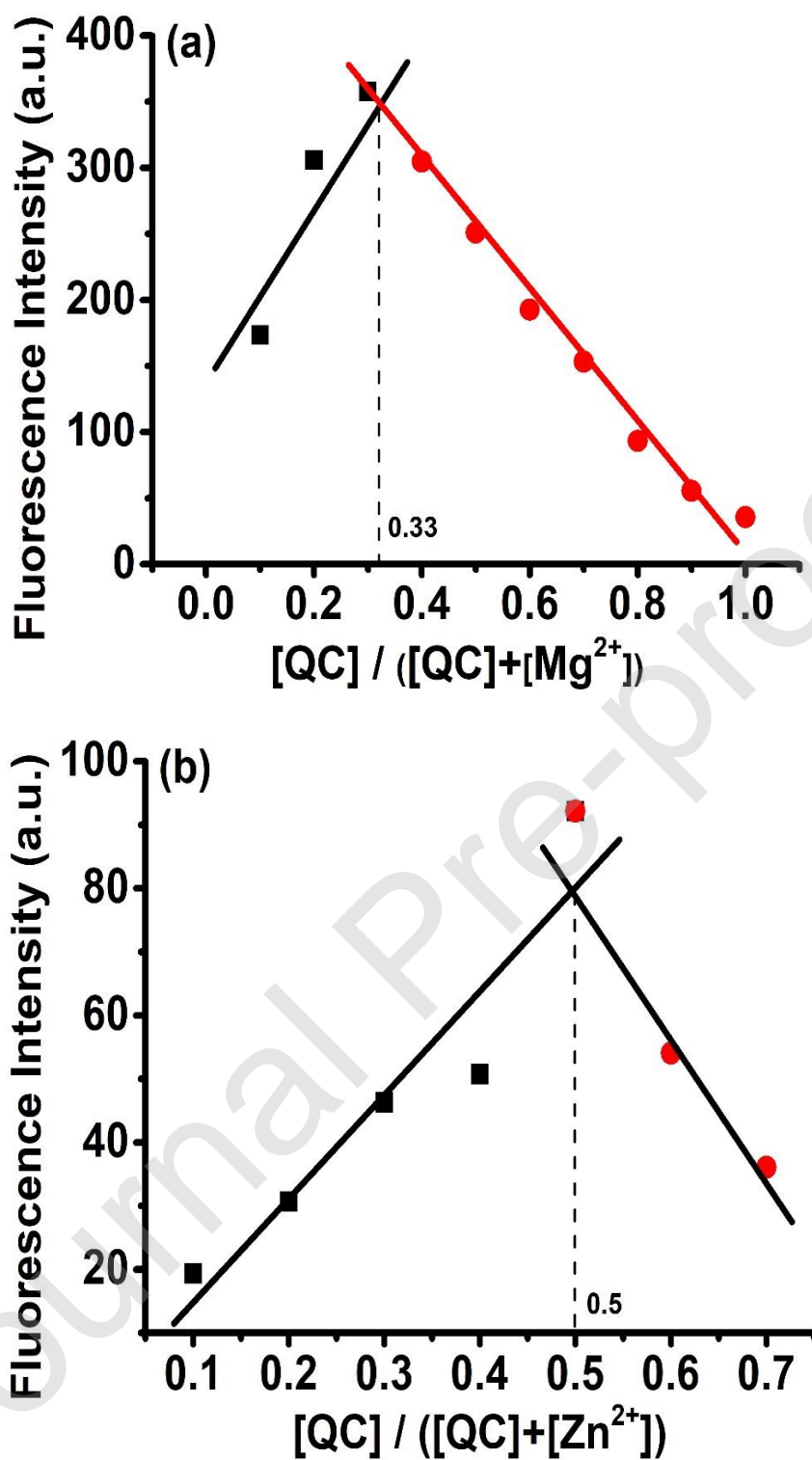


Figure 5. (a) Job's plot of  $\text{QC}+2\text{Mg}^{2+}$  system in acetonitrile ( $[\text{QC}] + [\text{Mg}^{2+}] = 10.0 \mu\text{M}$ ). (b) Job's plot of  $\text{QC}+\text{Zn}^{2+}$  system in EtOH-H<sub>2</sub>O (9:1, v/v) ( $[\text{QC}] + [\text{Zn}^{2+}] = 10.0 \mu\text{M}$ ).

## 3.5 Computational studies

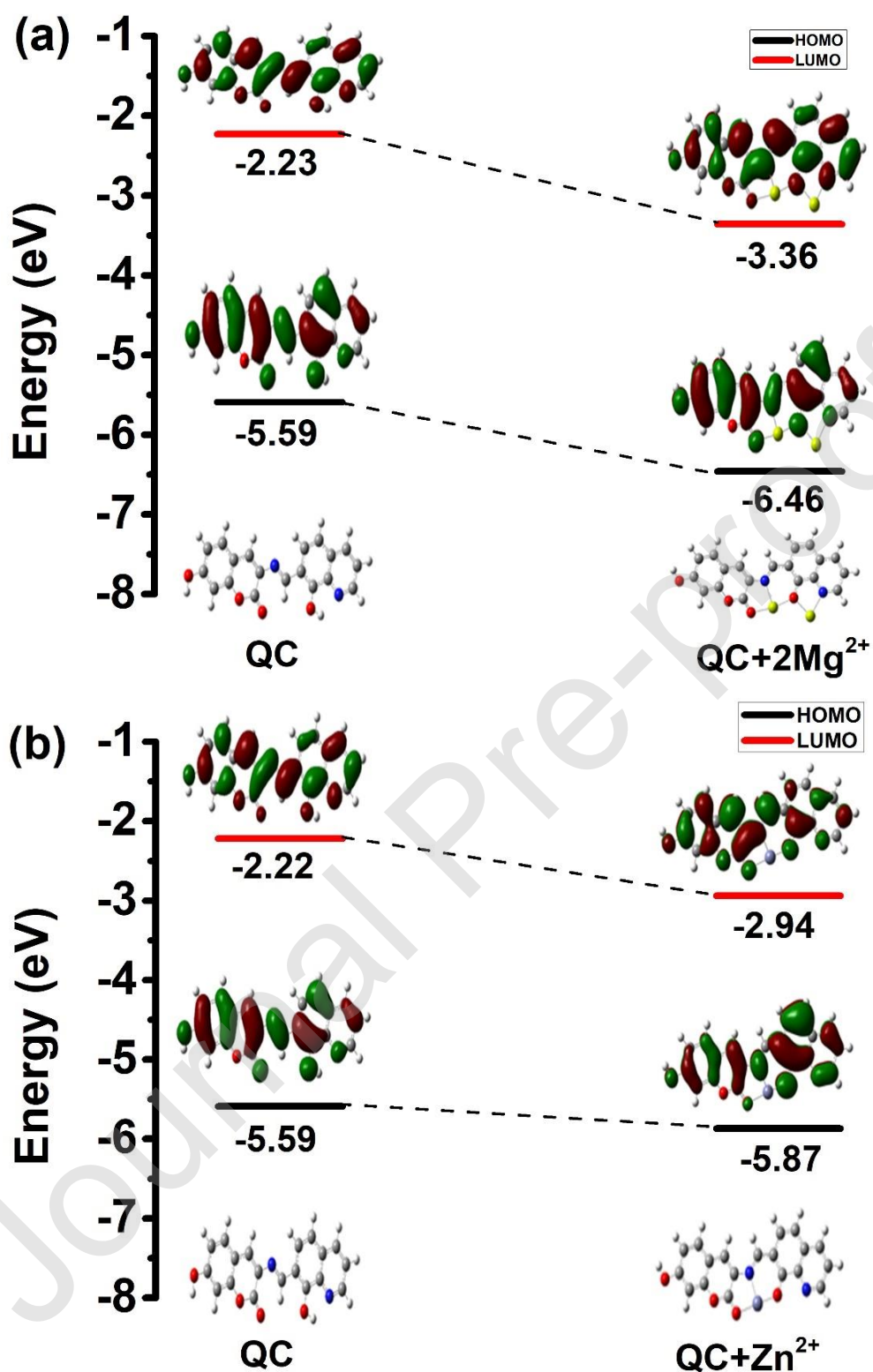


Figure 6. Optimized structures, HOMO–LUMO energy levels, and the molecular orbital plots: (a) QC and QC +  $2\text{Mg}^{2+}$ . (b) QC and QC +  $\text{Zn}^{2+}$ .

To better understand the recognition mechanism of **QC** toward  $\text{Mg}^{2+}$  ion or  $\text{Zn}^{2+}$  ion, DFT (density functional theory) computations were performed on the Gaussian 09 program, and the B3LYP/6-31G(d) basis set was used for optimizing the structure [31]. First, acetonitrile was selected for the system of **QC** +  $2\text{Mg}^{2+}$ , as shown in Figure 6a, with the treatment of  $\text{Mg}^{2+}$  ion, the results showed that the electron densities of both HOMOs and LUMOs are mainly distributed at the **QC**, and therefore the complex showed a fluorescence enhancement due to a smaller energy gap 3.10 eV than 3.36 eV of **QC**. In contrast, the calculation for **QC** +  $\text{Zn}^{2+}$  was conducted in EtOH, as can be seen from the Figure 6b, after the formation of 1:1 complex between **QC** and  $\text{Zn}^{2+}$  ion, the quinoline moiety served as HOMO while coumarin group act as LUMO in complex, indicating that ICT process occurred from quinoline moiety to coumarin group, the complex therefore mainly emitted the fluorescence peak of coumarin group and showed a fluorescence enhancement due to a smaller energy gap 2.93 eV than 3.37 eV of **QC**.

### 3.6 Proposed mechanism

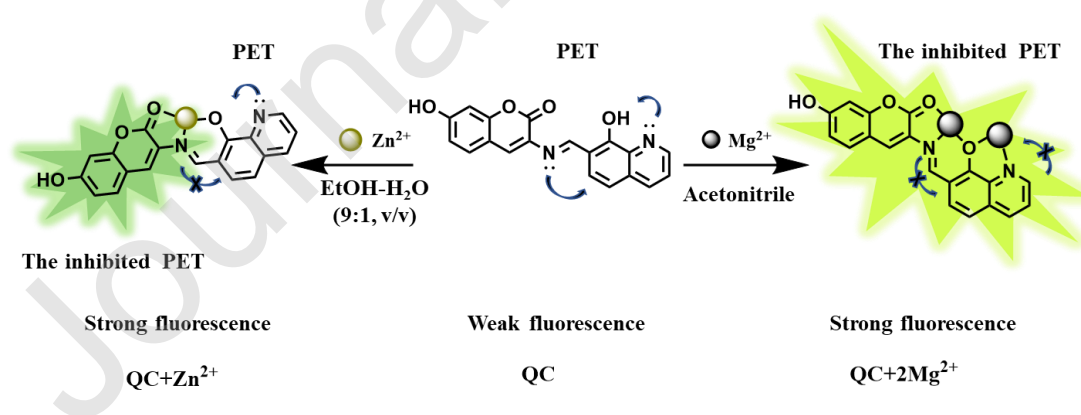


Figure 7. Proposed recognition mechanism of **QC** for  $\text{Mg}^{2+}$  and  $\text{Zn}^{2+}$

Based on the above results, a possible recognition mechanism was proposed as demonstrated in Figure 7. Whether in acetonitrile or EtOH- $\text{H}_2\text{O}$  (9:1, v/v), **QC** showed

a weak fluorescence emission at 525 nm or 530 nm due to the C=N isomerization and the photoinduced electron-transfer (PET) processes, which were caused by the lone pair electrons from the nitrogen atom of the -C=N group and the nitrogen atom of quinoline moiety. After the formation of the complex between **QC** and  $Mg^{2+}$  ion, C=N isomerization and the PET processes were inhibited completely, the conjugate plane structure of the rigidity was improved, resulting the fluorescence enhancement response of **QC** toward  $Mg^{2+}$  ion. However, for the detection of  $Zn^{2+}$  ion, fluorescence intensity of **QC** at 530 nm decreased first due to the 1:1 stoichiometric ratio between **QC** and  $Zn^{2+}$  ion, which inhibited the PET process caused by the nitrogen atom of the -C=N group and destroyed the fluorescence properties of **QC**. Then a new fluorescence peak at 520 nm appeared and increased with the addition of  $Zn^{2+}$  ion, which should be attributed to the characteristic emission of coumarin group rather than that of **QC**. Therefore, **QC** successfully served as a solvent-dependent fluorescent probe for dual selective detection of  $Mg^{2+}$  ion and  $Zn^{2+}$  ion.

#### 4. Conclusion

In summary, a simple solvent-dependent fluorescent probe **QC** for  $Mg^{2+}$  ion or  $Zn^{2+}$  ion has been constructed based on a Schiff base compound. Among the commonly metal ions, this probe showed highly selective detection of  $Mg^{2+}$  ion in acetonitrile and  $Zn^{2+}$  ion in EtOH-H<sub>2</sub>O (9:1, v/v), respectively. For  $Mg^{2+}$  ion, the fluorescence intensity of **QC** increased because the C=N isomerization and the PET processes were inhibited. For  $Zn^{2+}$  ion, however, the fluorescence intensity of **QC** decreased and a new fluorescence peak appeared, this was because the PET process caused by the nitrogen

atom of the -C=N group was inhibited and ICT process occurred from quinoline moiety to coumarin group, which was supported by DFT analysis. To the end, we hope this strategy can be employed to develop such multianalyte fluorescent probes in the future.

#### **Author statement**

**Jing-Can Qin:** Investigation, Methodology, Data curation, Writing-Original Draft

**Min Wang:** Investigation, Software, Writing - Review & Editing

**Zhen-Hai Fu:** Supervision, Writing - Review & Editing

**Zhi-Hong Zhang:** Project administration

#### **Conflict of Interest**

The authors declare that they have no known competing financial interests or personal relationships that could have appeared to influence the work reported in this paper.

#### **Acknowledgement**

We thank the Natural Science Foundation of Qinghai (Grant Nos. 2019-ZJ-954Q), the CAS “Light of West China” Program (Y810041019) and the Youth Innovation Promotion Association CAS (2018466).

#### **Appendix A. Supplementary data**

Supplementary data available: Spectral data, copies of  $^1\text{H}/^{13}\text{C}$  NMR and other materials can be found online at [http://doi.org/\\*\\*\\*\\*\\*](http://doi.org/*****).

#### **References**

- [1] L. Lvova, C. G. Goncalves, C. D. Natale, A. Legin, D. Kirsanov, R. Paolesse, *Talanta* 179 (2018) 430–441.
- [2] Y. Matsui, K. K. Sadhu, S. Mizukami, K. Kikuchi, *Chem. Commun.* 53 (2017)

10644–10647.

[3] R. Treadwell, F. D. Moliner, R. Subiros-Funosas, T. Hurd, K. Knox, M. Vendrell, *Org. Biomol. Chem.* 16 (2018) 239–244.

[4] T. Yu, P. Sun, Y. Hu, Y. Ji, H. Zhou, B. Zhang, Y. Tian, J. Wu, *Biosens. Bioelectron.* 86 (2016) 677–682.

[5] A. Pandey, A. Kumar, S. Vishwakarma, K. K. Upadhyay, *RSC Adv.* 6 (2016) 6724–6729.

[6] M.-H. Kao, T.-Y. Chen, Y.-R. Cai, C.-H. Hu, Y.-W. Liu, Y. Jhong, A.-T. Wu, *J. Lumin.* 169 (2016) 156–160.

[7] K. Chantalakana, N. Choengchan, P. Yingyuad, P. Thongyoo, *Tetrahedron Lett.* 57 (2016) 1146–1149.

[8] T.-T. Zhang, X.-P. Chen, J.-T. Liu, L.-Z. Zhang, J.-M. Chu, Su L, B.-X. Zhao, *RSC Adv.* 4 (2014) 16973–16978.

[9] Y. Zhang, B. Yuan, D. Ma, *Inorg. Chim. Acta* 508 (2020) 119640.

[10] M. Liu, X. Yu, M. Li, N. Liao, A. Bi, Y. Jiang, S. Liu, Z. Gong, W. Zeng, *RSC Adv.* 8 (2018) 12573–12587.

[11] P. Saluja, H. Sharma, N. Kaur, N. Singh, D. O. Jang, *Tetrahedron* 68 (2012) 2289–2293.

[12] S. Devaraj, Y. Tsui, C.-Y. Chiang, Y.-P. Yen, *Spectrochim. Acta, Part A* 96 (2012) 594–599.

[13] S. Dey, A. Maity, M. Shyamal, D. Das, S. Maity, P. K. Giri, N. Mudi, S. S. Samanta, P. Hazra, A. Misra, *Photochem. Photobiol. Sci.* 18 (2019) 2717–2729.

- [14] P. Ghorai, K. Pal, P. Karmakar, A. Saha, Dalton Trans. 49 (2020) 4758–4773.
- [15] S. Guang, G. Wei, Z. Yan, Y. Zhang, G. Zhao, R. Wu, H. Xu, Analyst 143 (2018) 449–457.
- [16] P. Wang, J. Wu, Spectrochim. Acta, Part A 208 (2019) 140–149.
- [17] J. Xue, L. Tian, Z. Yang, J. Photochem. Photobiol., A 369 (2019) 77–84.
- [18] K. Rout, A. K. Manna, M. Sahu, G. K. Patra, Inorg. Chim. Acta 486 (2019) 733–741.
- [19] P. S. Hariharan, N. Hari, S. P. Anthony, Inorg. Chem. Commun. 48 (2014) 1–4.
- [20] Y. Wang, P.-D. Mao, W.-N. Wu, X.-J. Mao, Y.-C. Fan, X.-L. Zhao, Z.-Q. Xu, Z.-H. Xu, Sens. Actuators, B 255 (2018) 3085–3092.
- [21] Y. Wang, W.-W. Wang, W.-Z. Xue, W.-N. Wu, X.-L. Zhao, Z.-Q. Xu, Y.-C. Fan, Z.-H. Xu, J. Lumin. 212 (2019) 191–199.
- [22] A. Dhara, N. Guchhait, I. Mukherjee, A. Mukherjee, S. C. Bhattacharya, RSC Adv. 6 (2016) 105930–105939.
- [23] R. Alam, T. Mistri, A. Katarkar, K. Chaudhuri, S. K. Mandal, A. R. Khuda-Bukhsh, K. K. Das, M. Ali, Analyst 139 (2014) 4022–4030.
- [24] X. Bai, J. Yan, J. Qin, Z. Yang, Inorg. Chim. Acta 474 (2018) 44–50.
- [25] Y. Li, J. Wu, X. Jin, J. Wang, S. Han, W. Wu, J. Xu, W. Liu, X. Yao, Y. Tang, Dalton Trans. 43 (2014) 1881–1887.
- [26] L. Wang, W. Qin, X. Tang, W. Dou, W. Liu, J. Phys. Chem. A 115 (2011) 1609–1616.
- [27] Y. Wang, Z.-G. Wang, X.-Q. Song, Q. Chen, H. Tian, C.-Z. Xie, Q.-Z. Li, J.-Y. Xu,

Analyst 144 (2019) 4024–4032.

[28] Z.-H. Fu, L.-B. Yan, X. Zhang, F.-F. Zhu, X.-L. Han, J. Fang, Y.-W. Wang, Y. Peng, Org. Biomol. Chem. 15 (2017) 4115–4121.

[29] M. Wang, Y.-M. Zhang, Q.-Y. Zhao, Z.-H. Fu, Z.-H. Zhang, Chem. Phys. 527 (2019) 110470.

[30] X. Yang, P. Cai, Q. Liu, J. Wu, Y. Yin, X. Wang, L. Kong, Bioorg. Med. Chem. 26 (2018) 3191–3201.

[31] Z.-H. Fu, Y.-W. Wang, Y. Peng, Chem. Commun. 53 (2017) 10524–10527.

[32] J. A. González-Vera, E. Luković, B. Imperiali, J. Org. Chem. 74 (2009) 7309–7314.

[33] J.-S. Wu, W.-M. Liu, X.-Q. Zhuang, F. Wang, P.-F. Wang, S.-L. Tao, X.-H. Zhang, S.-K. Wu, S.-T. Lee, Org. Lett. 9 (2007) 33–36.